

The Ultrafast Dynamics of Hydrogen-Bonded Liquids: Molecular Structure-Dependent Occurrence of Normal Arrhenius or Fractional Stokes–Einstein–Debye Rotational Diffusive Relaxation

Neil T. Hunt,^{*,†} Andrew R. Turner,[†] Hajime Tanaka,[‡] and Klaas Wynne[†]

Department of Physics, SUPA, University of Strathclyde, Glasgow G4 0NG, Scotland, United Kingdom, and Institute of Industrial Science, University of Tokyo, Meguro-ku, Tokyo 153-8505, Japan

Received: March 27, 2007; In Final Form: June 7, 2007

The ultrafast rotational-diffusive dynamics of the peptide linkage model compounds N-methylacetamide (NMA), acetamide (Ac), and N,N-dimethylacetamide (DMA) have been studied as a function of temperature using optically heterodyne-detected optical Kerr effect (OHD-OKE) spectroscopy. Both NMA and Ac exhibit a non-Arrhenius temperature dependence of the rotational diffusive relaxation time. By contrast, the non-hydrogen-bonding DMA exhibits normal hydrodynamic behavior. The unusual dynamics of NMA and Ac are attributed to the decoupling of single-molecule rotational diffusive relaxation from the shear viscosity via a transition between stick and slip boundary conditions, which arises from local heterogeneity in the liquid due to the formation of hydrogen-bonded chains or clusters. This provides new insight into the structure and dynamics of an important peptide model compound and the first instance of such a phenomenon in a room-temperature liquid. The OHD-OKE responses of carboxylic acids acetic acid (AcOH) and dichloroacetic acid (DCA) are also reported. These, along with the terahertz Raman spectra, show no evidence of the effects observed in amide systems, but display trends consistent with the presence of an equilibrium between the linear and cyclic dimer structures at all temperatures and moderate-to-high mole fractions in aqueous solution. This equilibrium manifests itself as hydrodynamic behavior in the liquid phase.

1. Introduction

Inter- and intramolecular hydrogen bonding plays an important role in determining the structure and function of biological molecules. As such, a thorough understanding of the interactions between molecules in hydrogen-bonded liquids is crucial to our comprehension and exploitation of biological systems. Studying intermolecular interactions in complete biological systems, however, is problematical due to the size and complexity of the molecules involved. This has resulted in the use of simpler model systems to further our understanding.

N-Methylacetamide (NMA, $\text{CH}_3\text{NHCOCH}_3$), which closely resembles the peptide linkage, is one such model system that has been extensively studied.^{1–15} The majority of this work has concentrated on determining the structure of NMA in the liquid phase and in solution. It has been suggested by theoretical simulations of liquid NMA that the molecules form hydrogen-bonded chain-like aggregates in the liquid phase similar to those found in the crystalline state.^{1,2} A variety of experimental approaches have been employed such as FTIR spectroscopy,^{8,9} including multidimensional correlation techniques,^{3–7} Raman scattering,^{2,9–11} and X-ray diffraction¹³ at a range of temperatures and levels of dilution in both hydrogen-bonding and non-hydrogen-bonding solvents. To date, however, a definitive picture of the intermolecular interactions in liquid NMA remains elusive. Studies of NMA using 2D correlation FTIR spectroscopy^{3–6} have yielded features that were assigned to hydrogen-bonded aggregates but it has also been suggested that

these may be due to temperature-induced frequency shifts of vibrational bands.⁷ Similarly, mid-infrared spectroscopy has been used to obtain quantitative estimates of the extent of NMA self-association but the values obtained vary considerably.^{8,9} The amide I band of NMA has been the focus of much study using both infrared and Raman spectroscopies.^{2,9–11} In some cases, sub-bands of this transition have been identified that have been attributed to the formation of aggregates.^{10,12} A gradual evolution of the shape and position of the amide I band with temperature or concentration was linked to changes in cluster sizes. Some evidence for short range order and self-association has also been obtained using X-ray diffraction in conjunction with density functional theory (DFT) calculations¹³ and measurements of the hydration enthalpy of NMA.¹⁴

Ultrafast spectroscopic methods have also been applied to the study of NMA. 2D-IR experiments produced a value of 10–15 ps for the hydrogen-bond lifetime of NMA dissolved in methanol-*d*₄,¹⁵ while recently we employed optically heterodyne-detected optical Kerr-effect (OHD-OKE) spectroscopy to determine the rotational diffusive dynamics and terahertz Raman spectrum of NMA at a range of temperatures and levels of dilution in water and CCl_4 .¹⁶ Unusual changes in the rotational relaxation time of NMA were observed contrary to established hydrodynamic theory for simple liquids. These were tentatively attributed to a model in which neat NMA forms hydrogen-bonded aggregates that break up at a critical temperature or dilution level. Accompanying changes in the low-frequency Raman and infrared transition intensities were also observed, which indicated the presence of collective effects that change the polarizability and dipole moment in a nonstoichiometric manner.¹⁶

* To whom correspondence should be addressed.

[†] University of Strathclyde.

[‡] University of Tokyo.

TABLE 1: Results of Fitting OHD-OKE Data to Eq 3 and Various Physical Constants Relating to the Studied Liquids; Shown Are the Melting Temperature, the Boiling Temperature, the Heat of Vaporization, the Viscosity at Room Temperature, and the Activation Energy Obtained through Fitting OHD-OKE Data to Eq 3

molecule	T_m^a (°C)	T_b^a (°C)	ΔH_{vap} (kJ mol ⁻¹)	E_a (K)	$\eta^{298\text{K}}$ (mPas)
N,N-dimethylacetamide (DMA)	20	165	50.2 ^b	736	1.927 ^c
N-methylacetamide (NMA) <393K	27	205	69.9 ^b	184	2.2
N-methylacetamide (NMA) >393K				1200	
acetamide (Ac) <425 K	78	221	80.3 ^b	750	
acetamide (Ac) >425 K				2760	
acetic acid (AcOH)	16	120	41.7 ^c	963	1.056 ^c
dichloroacetic acid (DCA)	10	194		462	

^a Sigma Aldrich data. ^b Della Gatta et al.⁷² ^c CRC Handbook, 89th ed.⁷³

Here, we have studied the behavior of neat liquid NMA at higher temperature resolution to determine more accurately the nature of the temperature-induced transition point in the rotational diffusive dynamics. These new data have been combined with differential scanning calorimetry (DSC) and measurements of the macroscopic liquid viscosity in order to shed further light on the origins of this unusual behavior.

The changes in the rotational diffusion time observed have several possible origins. These include a liquid–liquid phase transition between hydrogen-bonded and non-hydrogen-bonded states or an unusual temperature dependence of factors such as molecular volume, pairwise correlation effects, or in the coupling between macroscopic shear viscosity and microscopic molecular dynamics but to date the data are inconclusive. While liquid–liquid phase transitions (LLT) have been clearly observed for atomic liquids,^{17–21} direct experimental evidence for such phenomena in molecular liquids has only been reported very recently and often close to the glass transition or freezing point

of the liquids concerned.^{22,23} It has been shown, however, that the possibility exists for an LLT in any molecular liquid that has a tendency to form long-lived locally favored structures due to anisotropic interactions such as those arising from hydrogen bonds.^{23,24}

Examples of non-Arrhenius temperature dependencies of rotational relaxation times have been observed previously. The origins of such phenomena are largely due to microscopic heterogeneities in the liquid structure, which enable the decoupling of molecular reorientation from the macroscopic liquid viscosity.^{25–27} Most relevant to this work is the recent observation of fractional Stokes–Einstein behavior in pure liquid HF.²⁵

We have investigated other hydrogen-bonded systems; two further amides have been studied in an effort to determine whether the effects observed for NMA also occur in liquids with similar structural motifs. The systems chosen were the non-hydrogen-bonding N,N-dimethylacetamide (DMA) along with acetamide (Ac), which has the capacity to form two intramolecular hydrogen bonds via the amide nitrogen. The model compound formamide was not studied although it may be expected to behave similarly to Ac.²⁸

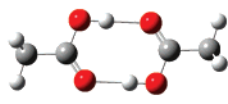
In addition, we have studied acetic acid (AcOH) and the derivative dichloroacetic acid (DCA) to judge whether these effects occur in other hydrogen-bonding systems. Acetic acid has been the subject of much debate regarding its structure and intermolecular hydrogen bonding. While it is now widely accepted that the crystalline form is based upon linear hydrogen-bonded chains^{29–36} and the gas phase is dominated by the so-called cyclic dimer (see Table 2 for structures),³⁷ the structure of the liquid phase remains a topic of much debate. Following studies using Raman scattering and FTIR spectroscopy at a range of temperatures and pressures, it is now widely agreed that neat acetic acid consists mainly of an equilibrium between cyclic and linear dimers.^{38–40} The situation in aqueous solution is less

TABLE 2: Results of DFT Calculations on AcOH and DCA Monomer and Dimer Structures

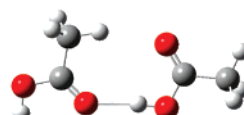
	Experiment (cm ⁻¹)	Monomer I (cm ⁻¹)	Cyclic Dimer II (cm ⁻¹)	Linear Dimer III (cm ⁻¹)	Assignment
AcOH	~ 40 (br)	57	49	55 & 103	Me torsion
	~ 120 (br)		120	92	oop H-bond bend
			160	114	ip H-bond bend
	446	425	175	433 & 446	ip H-bond bend C-C-O bend
DCA	~ 50 (br)	36	23	33 & 57	CO ₂ torsion
			66		oop H-bond bend
	~ 150 (br)		93	81	ip H-bond bend
			138	116	ip H-bond bend
	205	183	215	182 & 195	asym C-C-Cl ₂ bend
	247	230	265	221 & 240	sym C-C-Cl ₂ bend
			283		Cl-C-Cl bend
	420	401	416	421	C-C-O bend

Energies/Structures

AcOH = -229 au
DCA = -1148 au



AcOH = -458 au
DCA = -2296 au



AcOH = -458 au
DCA = -2296 au

clear, however. It has been suggested that acetic acid–water mixtures form two microphases: a water cluster phase at high water concentrations and an acetic acid cluster phase consisting mainly of chain clusters similar to those found in the crystalline phase.^{41,42} More recently, attenuated total reflectance (ATR) FTIR spectroscopy has been combined with Raman scattering and ab initio calculations to suggest that acetic acid exists as a hydrated monomer at low concentrations (<1 M) and that, as the mole fraction increases, the populations of linear dimers and subsequently cyclic dimers increase steadily.³⁸

We have studied the rotational-diffusive dynamics and terahertz Raman spectrum of AcOH and DCA as a function of temperature. As a result of the chlorine atoms present in DCA, the low-frequency spectra feature some modes that can be used to report on the hydrogen-bonded state of the molecule. Changes observed in these modes at elevated temperature were studied as a function of aqueous dilution. Density functional theory (DFT) calculations were employed in an effort to fully characterize the behavior of these systems.

The remainder of the paper is organized as follows: section 3 contains details of the experiments carried out. The results are presented in section 4, followed by a discussion in section 5, and finally, a summary is presented and conclusions drawn.

2. Experimental

The OHD-OKE method is well established and has been widely used to measure the third-order polarizability anisotropy of a wide range of liquid samples.^{43–45} This method has been used extensively to study the dynamics of pure liquids and binary mixtures⁴⁵ and is increasingly being employed in investigations of more complex liquid-phase systems.⁴⁶ Examples of the latter include ionic liquids,^{47–49} microemulsions,^{50–53} sol–gel confined liquids,^{54–57} liquid crystals,^{58–61} polymers,^{62–65} biopolymers, and proteins.^{66–68} More recently, we have applied the technique to study the dynamics of hydrogen-bonded liquid systems.^{16,69} Fourier-transform deconvolution of the OHD-OKE response yields the low-frequency Raman spectral density.⁴⁵ The OHD-OKE spectrometer used has been described in detail elsewhere, as have the methods for Fourier transform deconvolution of the time-domain data.⁶⁹

The high-resolution temperature-dependent experiments on NMA were carried out by replacing the temperature control unit used previously to heat the copper cuvette holder (accuracy ± 5 K) with a DC source that could be controlled to an accuracy of ± 0.5 K.

All chemicals were obtained from Sigma-Aldrich Co Ltd and were used without further purification. All samples used for OHD-OKE spectroscopy were placed in cuvettes under a nitrogen atmosphere and sealed to prevent water contamination due to the hygroscopic nature of some of the molecules studied. The samples were filtered using 0.2 μm filters, and allowed to stand for 24 h prior to use.

Rheological measurements were made by a rheometer (Rheologica, Dynalysers VAR-CF) using a cone-plate geometry with a cone angle of 1°. The temperature dependence of the viscosity was measured upon heating at a rate of 1 K min^{-1} . The viscosity was measured with a strain-controlled mode: the shear rate was controlled to be 10² s⁻¹. The edge of the sample was covered by silicone oil to prevent evaporation of NMA.

Calorimetric measurements were made using a differential scanning calorimeter (Mettler Toledo, DSC-822e). The heat flux was measured upon heating at a rate of 1 K min^{-1} using a complex (AC) heat capacity measurement mode.

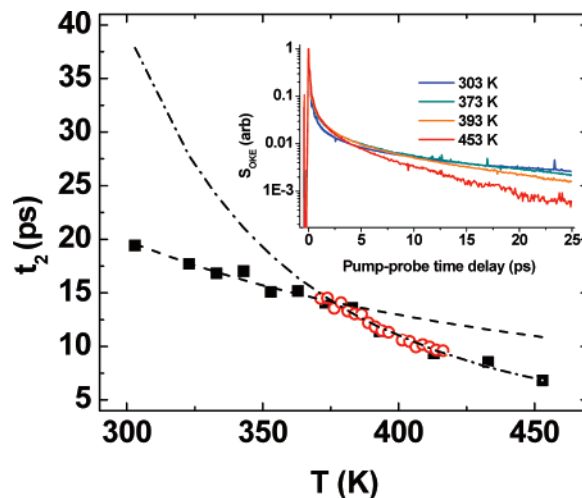


Figure 1. Temperature dependence of the OHD-OKE response of neat liquid NMA. The inset shows the OHD-OKE response of neat NMA in the time domain. The main picture shows the temperature dependence of the rotational-diffusive time scale of NMA. Black squares indicate previously published data¹⁶ while red circles indicate new data points. Dash-dot and dashed lines are fits to Arrhenius-type behavior above and below 383 K respectively.

All DFT calculations have been carried out using the Gaussian03 package.⁷⁰ Gas-phase DFT structure optimizations have been performed for AcOH and DCA in the monomer, cyclic dimer, and linear dimer forms using the B3LYP hybrid functional⁷¹ and the 6-311G++ basis set.⁷⁰ The optimized structures were then used as the basis for vibrational normal-mode calculations, which included the generation of Raman-scattering intensities.

3. Results and Discussion

N-Methylacetamide (NMA). The OHD-OKE response of NMA as a function of temperature is shown in Figure 1 (inset). In the time domain, the data are characterized by a sharp spike at zero pump–probe time delay attributable to the electronic hyperpolarizability of NMA. Between 50 and 250 fs, a shoulder is observed corresponding to librational motion of the NMA molecules. Beyond 1 ps, the data take on the form of a biexponential decay indicative of rotational-diffusive relaxation. This can be investigated quantitatively by fitting the OHD-OKE data at time delays greater than 1.5 ps to

$$r_{\text{diff}} = (a_1 e^{-t/t_1} + a_2 e^{-t/t_2})(1 - e^{-2\omega_{\text{av}}t}) \quad (1)$$

which has been shown to describe the picosecond dynamics of many simple liquids.⁴⁵ The results of this process are shown in Figure 1. In the case of a normal hydrodynamic fluid, the rotational-diffusive time scale (t_2) can be related to the shear viscosity (η) through the Stokes–Einstein–Debye (SED) relation:

$$t_2 = \frac{g_2 V \eta}{k_B T} \quad (2)$$

Here, t_2 is the collective reorientation time from OHD-OKE; g_2 is the static orientational pair correlation parameter, and V the hydrodynamic volume.

The shear viscosity of NMA as a function of temperature has been measured (see Figure 2a) and found to be consistent with a normal hydrodynamic liquid, i.e., the viscosity varies with temperature according to an Arrhenius function $\eta = A \exp(-E_a/k_B T)$, where $E_a/k_B \sim 1500$ K. Combining this Arrhenius

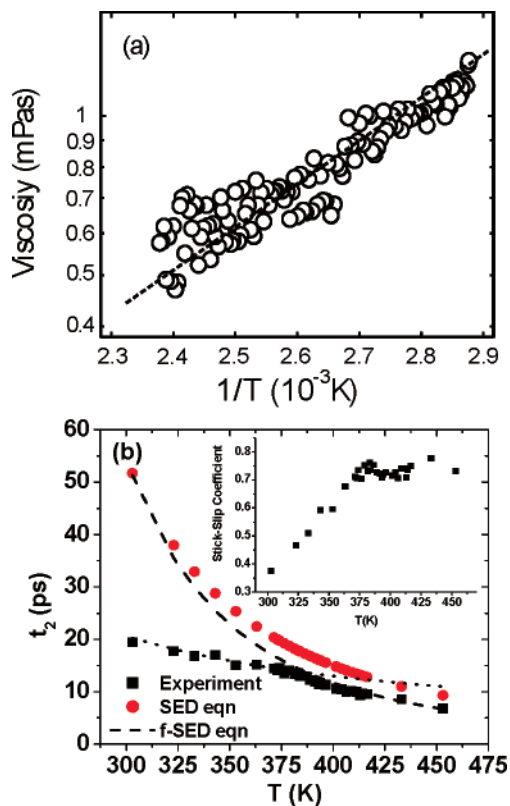


Figure 2. (a) Temperature dependence of the shear viscosity of pure liquid NMA. The dashed line shows a fit to an Arrhenius expression (see text). (b) Comparison of the t_2 values obtained via the OHD-OKE experiment and calculated using the SED equation. The inset shows the temperature variation of the stick-slip coefficient δ (see text). Dashed and dotted lines show fits to fractional DSE equation (see text). The dashed line has a ξ value of 1.04, the dotted line 0.3.

behavior of the viscosity with the SED expression eq 2, one would expect the rotational time scale of NMA to be well described by a function of the form

$$t_2 = \frac{A'}{T} \exp\left(\frac{E_a}{T}\right) \quad (3)$$

It was attempted to fit eq 3 to the temperature-dependent data in Figure 1 but it was found that one such profile was insufficient to fit the data across the complete range of temperatures at which NMA is a liquid (see dashed line Figure 1). The function failed to replicate the sudden deviation in the rotational relaxation time observed near 383 K. However, the t_2 value appears to follow two separate Arrhenius profiles, the first at temperatures below 383 K (dashed line Figure 1) and the second from 383 K upward (dash-dot line Figure 1). The parameters obtained from the fit are shown in Table 1.

There are three possible reasons for the unusual behavior of NMA, all of which have their origins in the hydrogen-bonding nature of the liquid. The deviation from Arrhenius behavior could be caused by: (1) a liquid–liquid phase transition (LLT); (2) an unusual temperature dependence of the parameters in the SED equation, such as g_2 or V ; or (3) a change in the boundary conditions that govern the coupling of the motion of NMA molecules in the liquid to the shear viscosity.

If a LLT were occurring between hydrogen-bonded and non-hydrogen-bonded states of NMA, it would be expected that an additional peak would be observed in the DSC profile of NMA at around 383 K. However, in DSC experiments carried out on dry NMA, no peak was observed and the temperature depen-

dence of the heat flux was observed to be monotonic. There was no distinct change around 383 K. These results exclude the possibility of the existence of a thermodynamic transition such as a liquid–liquid phase transition. It should be noted that small peaks in the DSC profile of liquid NMA have been reported previously at around 390 K¹¹ but in light of our results these would appear to have been caused by water contamination of the hygroscopic sample. It should be stressed that the OHD-OKE data were recorded using dry NMA under a nitrogen atmosphere and as such water contamination is not responsible for the observed change in the dynamics.

The possibility of the parameters of the SED equation displaying unusual temperature behavior is worthy of consideration. It can be envisaged that, at elevated temperatures, the break up of hydrogen-bonded aggregates may lead to a reduction in the value of the molecular volume or g_2 , the static orientational pair correlation parameter, which measures the degree of parallel ordering in the liquid and has a value of unity or greater.⁷⁴ A reduction in either of these at high-temperature would lead to reduced values of t_2 . However, such an occurrence would be expected to be observed in the macroscopic shear viscosity of the sample. Indeed, calculations of g_2 from the t_2 values measured through OHD-OKE, the experimental shear viscosities, and using the molecular volume of NMA, yielded unphysical g_2 values less than unity.

It is interesting to consider the results of fitting the observed t_2 values to eq 3 (see Table 1). In particular, the fact that the activation energy obtained at high temperature is significantly closer to that obtained through measurements of the shear viscosity than that at low temperature. This indicates that the measured rotational diffusion time is most strongly coupled to the shear viscosity at elevated temperatures. This suggests that the observed unusual behavior may be due to a transition between stick and slip boundary conditions²⁷ upon reducing the temperature. This effect has been observed for large probe molecules dissolved in glass-forming liquids,^{26,27} whereby at high temperatures the rotational dynamics of the probe closely follow the shear viscosity, but at low temperatures, local heterogeneities in the solvent enable the probe to rotate faster than the viscosity would appear to allow. This scenario is modeled using a variant of the SED equation employing slip boundary conditions, where $t_2^{\text{exp}} = \delta t_2^{\text{SED}}$. In this case, δ is less than unity and can be related to the shape of the molecular probe.⁷⁵

The results of examining the data from Figure 1 using this approach are shown in Figure 2b. Using the value of E_d/k_B from high-temperature portion of the NMA data, which is close to that obtained via the shear viscosity measurements (especially in light of the scatter on these results), a comparison of the calculated t_2^{SED} with the observed t_2^{exp} shows that the two are in close agreement above 383 K, leading to a δ value close to unity, indicating stick boundary conditions. Below 383 K, the values diverge suggesting that the observed t_2 is smaller than the shear viscosity would imply. This decoupling of t_2 from the viscosity may be brought about by the formation of a heterogeneous liquid structure through the formation of hydrogen-bonded chains. The observed t_2 values are then for NMA molecules not involved in chains, which will experience significantly decreased rotation-diffusion timescales.

Such decoupling of the rotational relaxation time and the viscosity has been observed previously^{26,76–80} and has also been discussed in terms of a variant of the SED equation referred to as the fractional SED equation.⁸¹ The f-SED equation features a power law dependence of η/T with the exponent ξ being unity

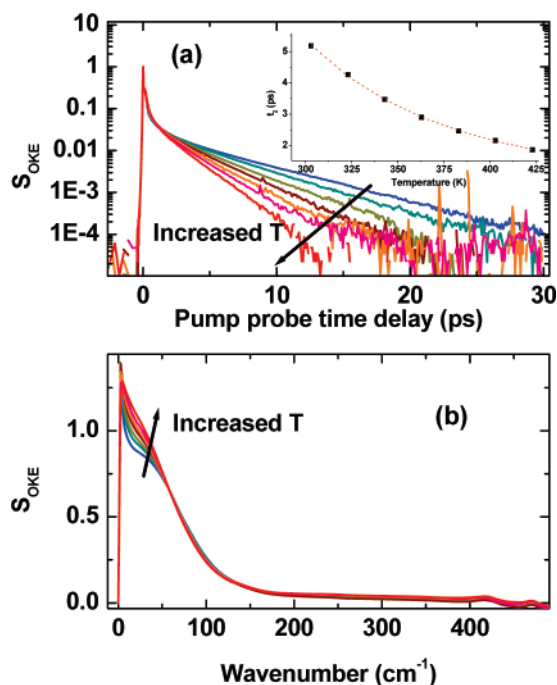


Figure 3. (a) Temperature dependence of the OHD-OKE response of neat DMA. The inset shows the results of fitting to a single Arrhenius profile (see text). (b) Terahertz Raman spectrum of neat DMA as a function of temperature.

for normal SED behavior and less than one in a decoupled system. The data in Figure 2(b) can be well represented by this relation even when using the experimental value for the activation energy of the shear viscosity (1500 K). Above 383 K, ξ had a value of 1.04 while below 383 K the value of ξ fell to 0.3. This representation of the data is more successful than that using the parameter δ above as it describes the data at all temperatures whereas the stick-slip approach implies increasing levels of “slippage” as the temperature decreases below 383 K (Figure 2b inset).

N,N-Dimethylacetamide (DMA). In order to put the results of NMA into context, the OHD-OKE response of neat DMA was recorded as a function of temperature between room temperature and the boiling point at 438 K. Once again, eq 1 was used to fit the time profiles and the results are shown in Figure 3a.

In contrast to NMA, DMA is unable to form intermolecular hydrogen bonds due to the absence of the peptide-like hydrogen atom. It is therefore interesting to note that the value of t_2 obtained for DMA near room temperature is nearly a factor of 4 lower than that of NMA despite the similar molecular size and viscosity (the room-temperature viscosities of NMA and DMA are given in Table 1). Additionally, the temperature dependence of t_2 for DMA shows no unusual behavior and can be reproduced using a single Arrhenius profile across the entire temperature range in which the liquid phase exists. This can be seen in the inset of Figure 3a while the parameters are given in Table 1. The reason for the differences in t_2 observed between NMA and DMA are likely to have their origins in hydrogen bonding. That the rotational-diffusion time scale for NMA is significantly longer despite the similar viscosities and molecular volumes would seem to indicate a larger g_2 parameter for NMA. This is reasonable, as the hydrogen bonding in NMA would promote parallel ordering and correlation effects absent in DMA. Similarly, the lack of hydrogen bonding in DMA accounts for the normal hydrodynamic behavior. The inability to form

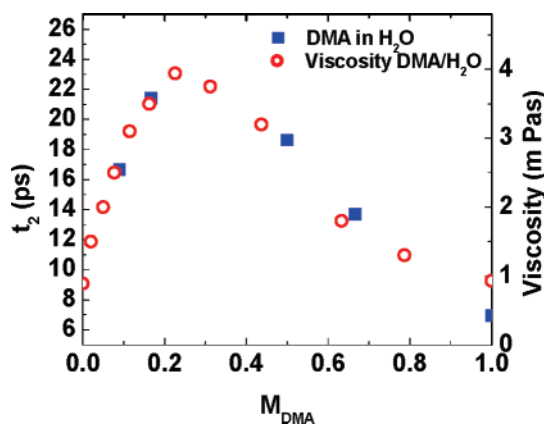


Figure 4. Rotational-diffusion time scale (t_2) of DMA as a function of aqueous dilution (blue squares) as compared to the viscosity of the solutions (red circles).⁸²

clusters or chains means that the liquid has no heterogeneous character at low temperature.

Fourier-transform deconvolution of the OHD-OKE response yields the terahertz Raman spectrum.⁶⁹ The results of this process for DMA are shown in Figure 3(b). Very little change is observed in the low-frequency Raman spectrum other than a slight narrowing of the broad librational band below 100 cm^{-1} and an increase in the scattering intensity at very low frequencies ($< 50 \text{ cm}^{-1}$). This is as observed previously for NMA,¹⁶ which also showed no substantive changes in the frequency domain spectrum. The narrowing of the librational band can be attributed to slight decreases in the liquid density at elevated temperatures, which leads to a slightly shallower intermolecular potential well and reduced frequency. In the case of DMA, the changes in the low-frequency scattering intensity can be attributed to the changes in the rotational-diffusion time scale leading to a broader contribution from the rotational-diffusive dynamics at low frequency. This was confirmed via subtraction of the rotational-diffusive component from the time domain data prior to Fourier transformation, although it is noted that the inherent assumption that such similar librational and rotational-diffusive timescales are separable is unlikely to be wholly accurate.

It was noted previously that the rotational-diffusive time scale of NMA exhibited sharp changes as a function of dilution in water.¹⁶ These were again attributed to a transition between the existence of hydrogen-bonded aggregates of NMA at high solute concentration and fully solvated NMA at mole fractions below 0.125. The study was repeated using DMA at a similar range of mole fractions and the results can be seen in Figure 4.

The results are as expected for the solvation of a non-hydrogen-bonding liquid in an aqueous solvent that can form hydrogen bonds to it.⁸² As the mole fraction of DMA increases, hydrogen bonds form between the solvent and solute leading to an increase in the viscosity, which peaks at an M_{DMA} value of around 0.25 before decreasing. It can also be seen from Figure 4 that the rotational-diffusion time of DMA dissolved in water closely follows the viscosity profile,⁸² as would be expected for a fluid that obeys the SED relation.

In the frequency domain, once again, no substantive changes to the Raman spectrum were observed with increased dilution other than a change in scattering intensity that was directly proportional to the mole fraction of DMA. This is as would be expected because the intensity of the OHD-OKE response is dependent upon the molecular polarizability. The signal from water is negligible compared to that of DMA and so the responses from the mixtures are dominated by that of DMA.

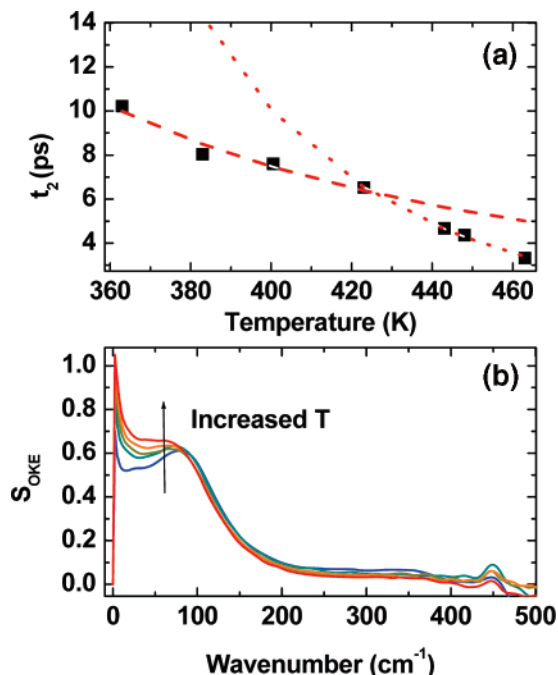


Figure 5. (a) Temperature dependence of the rotational-diffusion time of neat acetamide. Red lines indicate fitting to Arrhenius profiles (see text). The dotted line shows the results of fitting to the high-temperature portion of the data while the dashed line corresponds to the low-temperature results. (b) Terahertz Raman spectrum of acetamide as a function of temperature.

Taking the DMA data as a function of temperature and dilution as a whole it appears that, in the absence of intermolecular hydrogen bonding, DMA behaves as a normal hydrodynamic liquid, displaying none of the unusual behavior observed in NMA.

Acetamide (Ac). In contrast to both NMA and DMA, Ac has two available amide hydrogen atoms through which it can form intermolecular hydrogen bonds. This additional hydrogen-bonding capability not only offers the opportunity for forming three-dimensional hydrogen-bonded networks but also accounts for the fact that the melting point of Ac lies at 352 K, some 50 K above that of NMA and 100 K above DMA (Table 1). The OHD-OKE response of Ac as a function of temperature has been obtained. The results of fitting to eq 1 are shown in Figure 5. The elevated melting point of Ac means that the temperature range over which it could be studied was restricted by the heating system employed to between 352 and 463 K (Ac boils at 495 K), but it can be seen from the data that Ac shows non-single Arrhenius-type behavior with a transition point at around 425 K (parameters for the fits are given in Table 1). This behavior would appear to be consistent with that observed for NMA, which also forms intermolecular hydrogen bonds. Unfortunately, viscosity data for Ac are not available for further analysis.

The terahertz Raman spectra for Ac as a function of temperature are shown in Figure 5b. As with DMA, little change is observed although the increased amplitude at low frequencies due to the changing rotational-diffusive time scale is again observed. In the case of Ac, this is somewhat clearer as a result of the higher frequency of the librational band in comparison to that of DMA (100 cm^{-1} vs 50 cm^{-1}), leading to greater separation of the contributions. That the librational band of Ac lies at higher frequency can be attributed to the increased levels of intermolecular interaction through hydrogen bonding in comparison to DMA. It is noteworthy that the same band for

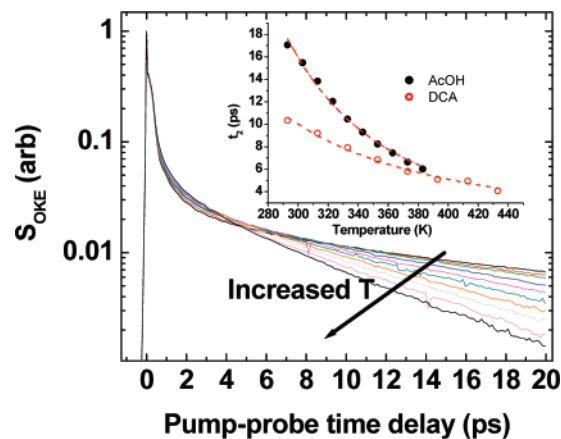


Figure 6. OHD-OKE response as a function of temperature for AcOH. Inset: plot of rotational-diffusion time vs temperature for AcOH and DCA; dashed red lines indicate the results of fitting to an Arrhenius profile.

NMA is located at around 80 cm^{-1} , which is consistent with the trends in hydrogen bonding ability and melting temperature of the three liquids. In the case of Ac, the librational band also narrows and shifts to lower frequency as the temperature is increased, consistent with expected changes in liquid density.

Acetic Acid (AcOH). It is instructive to extend the study to other types of hydrogen-bonding liquids in order to judge whether the effects observed for the amides, NMA and Ac above, are restricted to these systems. The results may also be able to shed some more light on the complex nature of the structure of the liquid phase of AcOH.

The OHD-OKE response of AcOH as a function of temperature is shown in Figure 6 with the results of fitting the data to eq 1 in the inset. It can clearly be seen that the data for AcOH shows simple hydrodynamic behavior as the rotational-diffusion time follows a single Arrhenius-type profile over the full temperature range of the liquid phase. This is interesting in light of the results for NMA and Ac but perhaps not surprising given that the structure of the liquid is expected to be a dynamic equilibrium between linear and cyclic dimers. If chain formation through polymerization of the linear dimer does not constitute a dominant fraction of the liquid, then hydrodynamic behavior would be expected.

As mentioned in the introduction, it is widely accepted that neat AcOH exists in an equilibrium between the cyclic and linear dimers at room temperature with the population of the linear dimer increasing with temperature. Therefore, it is interesting to examine the low-frequency response for any signs of changes in the population of these species. The results of the Fourier transformation process are shown in Figure 7a, and it can clearly be seen that very little change is observed in the low-frequency Raman spectrum of neat AcOH over the temperature range studied. The positions of the observed Raman bands are summarized in Table 2 along with the results of DFT calculations of the low-frequency Raman spectra of the monomer, cyclic dimer, and linear dimer structures. AcOH exhibits four main contributions to the terahertz Raman spectrum: the rotational-diffusive response at very low frequency ($<5\text{ cm}^{-1}$) and the librational band at around 40 cm^{-1} . In addition, intramolecular Raman modes are visible at 120 and 450 cm^{-1} . Previously, the latter has been attributed to a bending mode of the C-CO₂ group of the linear dimer,³⁸ that of the monomer being predicted nearer to 420 cm^{-1} ,³⁹ while the former has been assigned to several bands due to the bending and torsional motion of the ring component of the cyclic dimer.⁴¹ These

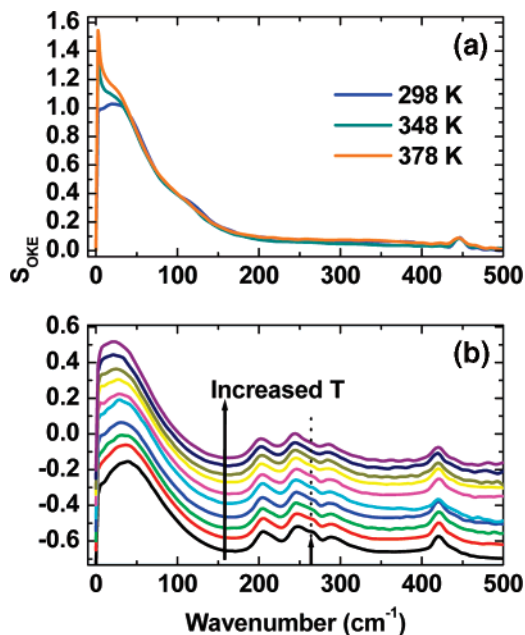


Figure 7. Terahertz Raman spectra of (a) neat AcOH and (b) neat DCA as a function of temperature.

observations are consistent with the results of the DFT calculations (Table 2). The C–CO₂ bend of the monomer is predicted to occur at 425 cm⁻¹ but at higher frequencies in the dimers. Similarly, both dimers show transitions in the 120 cm⁻¹ region that are not present in the predicted monomer spectrum. Differentiation between cyclic and linear dimers on the strength of DFT calculations is nontrivial because of the similarities of the results and the fact that the linear dimer has the capacity to polymerize needs to be considered also. However, these assignments seem to confirm the accepted notion that neat AcOH is composed of both linear and cyclic dimers, although there is little to suggest a change in the relative populations of these species with increased temperature. The fact that the equilibrium energies of the two dimer structures are significantly lower than that of the monomer is also persuasive.

Dichloroacetic Acid (DCA). Given the above results, it was decided to investigate the dichloro derivative of AcOH, which—due to the presence of the chlorine atoms—exhibits considerably more structure in the low-frequency region of the spectrum. These bands, while not directly involved in hydrogen bonding might be expected to act as reporter groups for the hydrogen-bonded state of the DCA molecule.

The results of the time-domain study of DCA are shown in the inset of Figure 6a, alongside those of AcOH. The two liquids show very similar temperature dependence of the OHD-OKE response as might be expected, with DCA also exhibiting normal hydrodynamic behavior throughout the liquid phase. That the rotational-diffusive time scale of DCA is shorter than that of AcOH may be due to slightly weaker hydrogen bonding as a result of the electron withdrawing effects of the chlorine atoms, a trend that is reflected in the melting temperatures of the two species (Table 1). Interestingly, this is not borne out in the boiling points, although increased dipolar interactions arising from the more polar DCA may explain this. Alternatively, the bulky chlorine atoms may inhibit the close packing of the molecules in DCA relative to AcOH leading to faster rotation rates.

The Raman spectrum of DCA as a function of temperature is shown in Figure 7b. In addition to the librational band located near 50 cm⁻¹, which once again shifts to lower frequency and

gains in intensity with increased temperature, there are several intramolecular modes of DCA present. The experimentally observed line positions and the results of DFT calculations on the DCA monomer and the cyclic and linear dimers are shown in Table 2.

As with AcOH, the observed spectrum of DCA seems to more closely resemble that predicted for the dimers rather than the monomer. The C–CO₂ band is observed at 420 cm⁻¹ close to the value calculated for both dimers, while that of the monomer is predicted to lie at lower frequency. Also, the broad contribution to the experimental spectrum near 150 cm⁻¹ is consistent with the flexing motions of the dimers and Raman scattering intensity at these frequencies is not predicted for the monomer. It should be noted that, as with AcOH, the broad nature of these bands in the low-frequency Raman spectrum is consistent with the inhomogeneous broadening associated with modes involving hydrogen bonds. The three modes observed between 205 and 290 cm⁻¹ are attributable to bending motions of the CCl₂ unit although it is difficult to draw any firm conclusions from the calculated positions of these modes due to the similar frequencies. That said, somewhat better agreement is seen between experiments and the predicted frequencies of the dimer modes than with those of the monomer.

In contrast to AcOH, increasing the temperature causes a change in the terahertz Raman spectrum of DCA. A shoulder located at 265 cm⁻¹, which is apparent at room temperature, decreases in intensity and apparently disappears by 373 K. While not a large enough change to indicate a dimer to monomer transition, this is indicative of a temperature-induced effect upon the liquid structure. Further analysis of these bands (presented in the Supporting Information), including studies of dilute solutions of DCA in water show that the changes are consistent with a dynamic equilibrium between the cyclic and linear dimers. Due to the spectral congestion however, it was possible neither to definitively assign contributions to individual structures, nor indeed to definitively exclude the possibility of the presence of small monomer contributions, but the patterns observed are consistent with previous studies of AcOH and AcOD implying that DCA does not behave in a significantly different manner.

General Discussion. It is interesting to consider the results of comparing the temperature dependence of the rotational-diffusive timescales of the liquids studied to the expected hydrodynamic models. In the case of DMA, AcOH, and DCA, the behavior was as expected, with all three showing a temperature-dependence that was well represented by a single Arrhenius-type profile. In contrast, NMA and Ac both showed behavior that could only be fitted using two such profiles. While non-single-Arrhenius behavior of the dynamics of molecular liquids such as that observed for NMA here is not a new phenomenon,^{26,76–80} it is, however, unexpected to observe this kind of effect in a pure room-temperature liquid. The observation of a crossover between two dynamical regimes is usually observed near a phase transition of the liquid, most typically near the glass transition point²⁷ or a similar fragile to strong transition where a liquid moves from a phase lacking short to medium range order to one where directional bonding predominates.⁸³

In the case of NMA, the macroscopic shear viscosity shows no deviation from the Arrhenius equation and measurements using DSC provided no evidence of a phase transition. This suggests that the non-Arrhenius behavior observed in OHD-OKE is due to a decoupling of the rotational relaxation time from the shear viscosity. Such an effect is well-known in

measurements of the relaxation dynamics of large dye probe molecules as the viscosity of the solvent increases.^{26,76–80} The origins of this effect lie in the increasing heterogeneity of the solvent as the temperature decreases, leading to the dye molecules not experiencing the shear viscosity but rather pockets of localized reduced viscosity enabling a faster rotational diffusive time scale than predicted by the SED equation. Such a transition from stick to slip boundary conditions is termed fractional SED behavior and is well described by the f-SED equation as shown above. This effect is also observed in the decoupling of translational motion though the effects are less marked than for rotational decoupling.^{84–89} This effect was not observed in pure molecular liquids until very recently.^{16,25} In both cases, the liquids were capable of hydrogen bond formation. In the case of HF, the value of ξ recovered was 0.02, reflecting the ability of the small molecule to rotate almost freely within the high viscosity liquid. The value obtained for NMA of 0.3 is consistent with that of 0.25 predicted for water.⁸¹ Similarly, values of 0.28 and 0.46 were obtained using ESR spectroscopy for the TEMPO radical in phenyl salicylate and ortoterphenyl.⁸⁰

It is worthy of note here that the terms stick and slip typically relate to the interaction of a probe molecule with a surrounding solvent and as such must be treated as effective terms when discussing pure liquids. The origin of f-SED phenomena arises from a decoupling of rotational motion of molecules from the macroscopic viscosity, which has been observed in pure HF²⁵ and is reported here for pure NMA and Ac. As such, the terms stick and slip are used to describe the dynamics of a population of the sample molecules that are rotating at a greater rate than the viscosity would seem to allow. This behavior in a hydrogen-bonded liquid can be explained by reference to a two state model,⁹⁰ similar to that applied effectively to water, in which the low energy state is characterized by directional hydrogen-bond interactions and the “excited” state by a lack of short to medium range order. As the temperature is reduced, the tendency to form locally ordered hydrogen-bonded structures increases leading to cluster formation. These clusters increase monotonically in size with decreasing temperature. In the case of NMA, this is exacerbated by cooperative effects, which encourage chain formation. Eventually the local heterogeneity increases to the point where a crossover to f-SED dynamics occurs. In light of this, it is not surprising that a similar effect is observed for Ac but not DMA. The involvement of hydrogen bonding is given further weight by the observation that, in the high-temperature (stick) regime, the Arrhenius activation energy of NMA corresponds to around 12.5 kJ mol⁻¹, which is close to the estimated strength of a hydrogen bond.

An implication of this is that the observed OHD-OKE relaxation arises from NMA molecules not involved in the formation of hydrogen-bonded chains and that there should be a contribution to the OHD-OKE signal from the relaxation dynamics of the chains, which would be expected to be significantly slower. It is thus necessary at this point to discuss the time scale of the experiments in comparison to the dynamics observed. The data for all samples were recorded and analyzed over pump–probe time delays of 30 ps, a value limited by the experimental arrangement and signal-to-noise ratios and as such, it must be considered whether this time scale has any direct effect upon the observed dynamics. As mentioned above, the OHD-OKE method has been widely used for studying the dynamics of liquid-phase systems and the fitting of the observed decay profiles to single or biexponential decay functions has been proved to be a useful approach to quantifying reorientational behavior, provided that each sample is subject to the same

time-window for analysis, as is the case here.^{43–46} Further, there exists no evidence that f-SED dynamics are observed as a result of experimental timescales that are comparable to the dynamics being studied. The above hypothesis is that the f-SED dynamics of NMA has its roots in heterogeneities in the liquid arising from the formation of hydrogen-bonded chains and as such, it would be expected that if the experiments were capable of being extended to longer timescales then a slower component would be observed arising from the relaxation of these chains. Such dynamics have been observed in polymers and liquid crystals,^{58,62,91} however work on polymer systems has shown that such signals are often weak⁵² in comparison to faster relaxation phenomena and at present are beyond the scope of the present spectrometer. Work is underway to address this, and it is anticipated that these data will form the basis of a future publication.

In light of these results, it is interesting to look in more detail at the data contained in Table 1. Taking the three amides as a group, it is clear that the melting temperatures, boiling temperatures, and heats of vaporization show the expected trend, increasing as the amount of intermolecular hydrogen bonding increases. Similarly, the activation energy obtained from the Arrhenius analysis increases with increasing hydrogen-bonding potential, but only if the high-temperature regime is used for the fitting. This is as would be expected if the trends in the rotational-diffusive times for Ac and NMA are caused by a transition to fractional SED behavior. In the high-temperature regime, the rotational dynamics are closely coupled to the viscosity giving a realistic value of E_a . Further, the fact that the value obtained for Ac is approximately double that of NMA mirrors the trends in the number of hydrogen bonds that each can form.

Looking at the data obtained for the acids studied, the fact that the two acids have similar melting points is as might be expected given their structural similarity. The heat of vaporization of DCA is unavailable, but given the close relationship between this and the melting point for both the amides and AcOH, it can be confidently predicted to be lower than that of AcOH. That no significant change in the structure of the acids is observed, accounts for the single-Arrhenius behavior of both liquids and the adherence to hydrodynamic predictions. This is in contrast to NMA and Ac, implying that the structure of the hydrogen bonded amides is disrupted at elevated temperatures.

Finally, it is interesting to speculate on whether such f-SED phenomena might be expected in other systems. The requirements, based upon the above results would seem to be the capability to form clusters or chains through locally ordered structures, which give rise to the inhomogeneity necessary for f-SED to occur. As such, this may be anticipated in the majority of hydrogen-bonding systems, including water. However, the temperature of the f-SED transition may not necessarily lie far from a glass or gel-transition point, making observation experimentally more difficult.

4. Conclusions

The high temperature behavior of the rotational-diffusive dynamics of NMA has been studied as a function of temperature close to a previously observed transition point.¹⁶ It has been established through measurements of the shear viscosity and heat flow via DSC experiments that the behavior is not due to a liquid–liquid phase transition but to a crossover transition to fractional Stokes–Einstein–Debye behavior at low-temperature caused by local heterogeneities in the liquid arising from the formation of hydrogen-bonded chains. This leads to the decou-

pling of the rotational relaxation time from the shear viscosity, an effect not previously observed in a pure room-temperature liquid. Similar behavior has been observed for Ac but not for the non-hydrogen-bonding DMA.

The study has been extended to AcOH and DCA to determine whether these hydrogen-bonded liquids behave in a similar manner. In both cases, simple hydrodynamic, Arrhenius behavior was observed for both liquids. Changes to the terahertz Raman spectra of DCA were observed, which were consistent with previous studies indicating that these molecules exist as an equilibrium between linear and cyclic dimer states. This equilibrium does not favor chain formation and results in normal, hydrodynamic behavior, in contrast to the hydrogen bonding amides.

Acknowledgment. The authors are grateful to R. Kurita and K. Murata for DSC and rheological measurements. This work was funded by EPSRC and the Leverhulme Trust (N.H., A.R.T., and K.W.) and by a grant-in-aid from the Ministry of Education, Culture, Sports, Science and Technology, Japan (H.T.). The authors would like to thank Austen Angell for very useful discussions and guidance in the area of glass forming liquids and liquid–liquid phase transitions. We would also like to thank Wouter Herrebut for assistance and discussions.

Supporting Information Available: Results of fitting the CCl_2 bending region of the Raman spectrum of neat DCA and DCA–water mixtures to six Gaussian profiles. This material is available free of charge via the Internet at <http://pubs.acs.org>.

References and Notes

- Whitfield, T. W.; Martyna, G. J.; Allison, S.; Bates, S. P.; Crain, *J. Chem. Phys. Lett.* **2005**, *414*, 210.
- Whitfield, T. W.; Martyna, G. J.; Allison, S.; Bates, S. P.; Vass, H.; Crain, *J. J. Phys. Chem. B* **2006**, *110*, 3624.
- Czarnecki, M. A.; Haufa, K. Z. *J. Phys. Chem. A* **2005**, *109*, 1015.
- Noda, I.; Liu, Y.; Ozaki, Y. *J. Phys. Chem.* **1996**, *100*, 8665.
- Noda, I.; Liu, Y.; Ozaki, Y. *J. Phys. Chem.* **1996**, *100*, 8674.
- Liu, Y.; Ozaki, Y.; Noda, I. *J. Phys. Chem.* **1996**, *100*, 7326.
- Huang, H.; Malkov, S.; Coleman, M.; Painter, P. *J. Phys. Chem. A* **2003**, *107*, 7697.
- Kuznetsova, L. M.; Furer, V. L.; Maklakov, L. I. *J. Mol. Struct.* **1996**, *380*, 23.
- Ludwig, R.; Reis, O.; Winter, R.; Weinhold, F.; Farrar, T. C. *J. Phys. Chem. B* **1998**, *102*, 9312.
- Schweitzer-Stenner, R.; Sieler, G.; Mirkin, N. G.; Krimm, S. *J. Phys. Chem. A* **1998**, *102*, 118.
- Herrebut, W. A.; Clou, K.; Desseyn, H. O. *J. Phys. Chem. A* **2001**, *105*, 4865.
- Schweitzer-Stenner, R.; Sieler, G.; Christiansen, H. *Asian J. Phys.* **1998**, *7*, 287.
- Trabelsi, S.; Bahri, M.; Nasr, S. *J. Chem. Phys.* **2005**, *122*, 024502.
- Akiyama, M. *Spectrochim. Acta, Part A* **2002**, *58*, 1943.
- Woutersen, S.; Mu, Y.; Stock, G.; Hamm, P. *Chem. Phys.* **2001**, *266*, 137.
- Hunt, N. T.; Wynne, K. *Chem. Phys. Lett.* **2006**, *431*, 155.
- Aasland, S.; McMillan, P. F. *Nature* **1994**, *369*, 633.
- Angell, C. A. *Science* **1995**, *267*, 1924.
- Poole, P. H.; Grande, T.; Angell, C. A.; McMillan, P. F. *Science* **1997**, *275*, 322.
- Mishima, O.; Stanley, H. E. *Nature* **1998**, *396*, 329.
- Katayama, Y.; Mizutani, T.; Utsumi, W.; Shimomura, O.; Yamakata, M.; Funakoshi, K. *Nature* **2000**, *403*, 170.
- Kurita, R.; Tanaka, H. *Science* **2004**, *306*, 845.
- Kurita, R.; Tanaka, H. *J. Phys.: Condens. Matter* **2005**, *17*, L293.
- Tanaka, H. *Phys. Rev. E* **2000**, *62*, 6968.
- Fernandez-Alonso, F.; Bermejo, F. J.; McLain, S. E.; Turner, J. F. C.; Molaison, J. J.; Herwig, K. W. *Phys. Rev. Lett.* **2007**, *98*, 077801.
- Blanchard, G. J.; Wirth, M. J. *J. Phys. Chem.* **1986**, *90*, 2521.
- Angell, C. A.; Ngai, K. L.; McKenna, G. B.; McMillan, P. F.; Martin, S. W. *J. Appl. Phys.* **2000**, *88*, 3113.
- Elola, M. D.; Ladanyi, B. M. *J. Chem. Phys.* **2006**, *125*, 184506.
- Wilmshurst, J. K. *J. Chem. Phys.* **1956**, *25*, 1171.
- Haurie, M.; Novak, A. *J. Chim. Phys.* **1965**, *62*, 137.
- Haurie, M.; Novak, A. *J. Chim. Phys.* **1965**, *62*, 146.
- Haurie, M.; Novak, A. *Spectrochim. Acta* **1965**, *21*, 1217.
- Foglizzo, R.; Novak, A. *J. Chim. Phys.* **1974**, *71*, 1322.
- Bertie, J. E.; Michaelian, K. H. *J. Chem. Phys.* **1982**, *77*, 5267.
- Fuji, Y.; Yamada, H.; Mizuta, M. *J. Phys. Chem.* **1988**, *92*, 6768.
- Nyquist, R. A.; Clark, T. D.; Streck, R. *Vibr. Spectrosc.* **1994**, *7*, 275.
- Derissen, J. L. *J. Mol. Struct.* **1971**, *7*, 67.
- Genin, F.; Quiles, F.; Burneau, A. *Phys. Chem. Chem. Phys.* **2001**, *3*, 932.
- Burneau, A.; Genin, F.; Quiles, F. *Phys. Chem. Chem. Phys.* **2000**, *2*, 5020.
- Semmler, J.; Irish, D. E. *J. Solution Chem.* **1988**, *17*, 805.
- Kosugi, K.; Nakabayashi, T.; Nishi, N. *Chem. Phys. Lett.* **1998**, *291*, 253.
- Nakabayashi, T.; Kosugi, K.; Nishi, N. *J. Phys. Chem. A* **1999**, *103*, 8595.
- Lotshaw, W. T.; McMorrow, D.; Thantun, N.; Melinger, J. S.; Kitchingham, R. *J. Raman Spectrosc.* **1995**, *26*, 571.
- Kinoshita, S.; Kai, Y.; Ariyoshi, T.; Shimada, Y. *Int. J. Mod. Phys., B* **1996**, *10*, 1229.
- Smith, N. A.; Meech, S. R. *Int. Rev. Phys. Chem.* **2002**, *21*, 75.
- Hunt, N. T.; Jaye, A. A.; Meech, S. R. *Phys. Chem. Chem. Phys.* **2007**, *9*, 2167.
- Giraud, G.; Gordon, C. M.; Dunkin, I. R.; Wynne, K. *J. Chem. Phys.* **2003**, *119*, 464.
- Xiao, D.; Rajian, J. R.; Li, S. F.; Bartsch, R. A.; Quitevis, E. L. *J. Phys. Chem. B* **2006**, *110*, 16174.
- Rajian, J. R.; Li, S. F.; Bartsch, R. A.; Quitevis, E. L. *Chem. Phys. Lett.* **2004**, *393*, 372.
- Hunt, N. T.; Jaye, A. A.; Meech, S. R. *J. Phys. Chem. B* **2003**, *107*, 3405.
- Hunt, N. T.; Jaye, A. A.; Meech, S. R. *Chem. Phys. Lett.* **2003**, *371*, 304.
- Hunt, N. T.; Jaye, A. A.; Hellman, A.; Meech, S. R. *J. Phys. Chem. B* **2004**, *108*, 100.
- Jaye, A. A.; Hunt, N. T.; Meech, S. R. *Langmuir* **2005**, *21*, 1238.
- Loughnane, B. J.; Farrer, R. A.; Scodinu, A.; Reilly, T.; Fourkas, J. T. *J. Phys. Chem. B* **2000**, *104*, 5421.
- Loughnane, B. J.; Farrer, R. A.; Scodinu, A.; Fourkas, J. T. *J. Chem. Phys.* **1999**, *111*, 5116.
- Farrer, R. A.; Loughnane, B. J.; Fourkas, J. T. *J. Phys. Chem. A* **1997**, *101*, 4005.
- Loughnane, B. J.; Fourkas, J. T. *J. Phys. Chem. B* **1998**, *102*, 10288.
- Gottke, S. D.; Brace, D. D.; Cang, H.; Bagchi, B.; Fayer, M. D. *J. Chem. Phys.* **2002**, *116*, 360.
- Gottke, S. D.; Cang, H.; Bagchi, B.; Fayer, M. D. *J. Chem. Phys.* **2002**, *116*, 6339.
- Hyun, B. R.; Quitevis, E. L. *Chem. Phys. Lett.* **2003**, *370*, 725.
- Hunt, N. T.; Meech, S. R. *J. Chem. Phys.* **2004**, *120*, 10828.
- Sengupta, A.; Terazima, M.; Fayer, M. D. *J. Phys. Chem.* **1992**, *96*, 8619.
- Sengupta, A.; Fayer, M. D. *J. Chem. Phys.* **1994**, *100*, 1673.
- Shirota, H.; Castner, E. W. *J. Am. Chem. Soc.* **2001**, *123*, 12877.
- Shirota, H.; Castner, E. W. *J. Chem. Phys.* **2006**, *125*, 034904.
- Giraud, G.; Wynne, K. *J. Am. Chem. Soc.* **2002**, *124*, 12110.
- Giraud, G.; Karolin, J.; Wynne, K. *Biophys. J.* **2003**, *85*, 1903.
- Hunt, N. T.; Kattner, L.; Shanks, R. P.; Wynne, K. *J. Am. Chem. Soc.* **2007**, *129*, 3168.
- Hunt, N. T.; Turner, A. R.; Wynne, K. *J. Phys. Chem. B* **2005**, *109*, 19008.
- Frisch, M. J.; Trucks, G. W.; Schlegel, H. B.; Scuseria, G. E.; Robb, M. A.; Cheeseman, J. R.; Montgomery, J. A., Jr.; Vreven, T.; Kudin, K. N.; Burant, J. C.; Millam, J. M.; Iyengar, S. S.; Tomasi, J.; Barone, V.; Mennucci, B.; Cossi, M.; Scalmani, G.; Rega, N.; Petersson, G. A.; Nakatsuji, H.; Hada, M.; Ehara, M.; Toyota, K.; Fukuda, R.; Hasegawa, J.; Ishida, M.; Nakajima, T.; Honda, Y.; Kitao, O.; Nakai, H.; Klene, M.; Li, X.; Knox, J. E.; Hratchian, H. P.; Cross, J. B.; Bakken, V.; Adamo, C.; Jaramillo, J.; Gomperts, R.; Stratmann, R. E.; Yazyev, O.; Austin, A. J.; Cammi, R.; Pomelli, C.; Ochterski, J. W.; Ayala, P. Y.; Morokuma, K.; Voth, G. A.; Salvador, P.; Dannenberg, J. J.; Zakrzewski, V. G.; Dapprich, S.; Daniels, A. D.; Strain, M. C.; Farkas, O.; Malick, D. K.; Rabuck, A. D.; Raghavachari, K.; Foresman, J. B.; Ortiz, J. V.; Cui, Q.; Baboul, A. G.; Clifford, S.; Cioslowski, J.; Stefanov, B. B.; Liu, G.; Liashenko, A.; Piskorz, P.; Komaromi, I.; Martin, R. L.; Fox, D. J.; Keith, T.; Al-Laham, M. A.; Peng, C. Y.; Nanayakkara, A.; Challacombe, M.; Gill, P. M. W.; Johnson, B.; Chen, W.; Wong, M. W.; Gonzalez, C.; Pople, J. A. *Gaussian 03*, revision B.05; Gaussian, Inc.: Wallingford, CT, 2004.
- Stephens, P. J.; Devlin, F. J.; Chabalowski, C. F.; Frisch, M. J. Ab initio calculation of vibrational absorption and circular dichroism spectra

using density functional force fields. *J. Phys. Chem.* **1994**, *98*, 11623–11627. Hertwig, R. H.; Koch, W. On the parameterization of the local correlation functional: What is Becke-3-LYP? *Chem. Phys. Lett.* **1997**, *268*, 345–351.

(72) Della-Gatta, G.; Barone, G.; Elia, V. *J. Solution Chem.* **1986**, *15*, 157.

(73) Lide, D. R. *CRC Handbook of Chemistry and Physics*; CRC Press: Boca Raton, FL, 2004.

(74) Zhu, X.; Farrer, R. A.; Fourkas, J. T. *J. Phys. Chem. B* **2005**, *109*, 12724.

(75) Hu, C.-M.; Zwanzig, R. *J. Chem. Phys.* **1974**, *60*, 4354.

(76) Jiang, Y.; Blanchard, G. J. *J. Phys. Chem.* **1994**, *98*, 6436.

(77) Megens, M.; Sprik, R.; Wegdam, G. H.; Lagendijk, A. *J. Chem. Phys.* **1997**, *107*.

(78) Hosoi, H.; Masuda, Y. *J. Phys. Chem. A* **1998**, *102*, 2995.

(79) Sluch, M. I.; Somoza, M. M.; Berg, M. A. *J. Phys. Chem. B* **2002**, *106*, 7385.

(80) Andreozzi, L.; Bagnoli, M.; Faetti, M.; Giordano, M. *J. Non-Cryst. Solids* **2002**, *303*, 262.

(81) Becker, S. R.; Poole, P. H.; Starr, F. W. *Phys. Rev. Lett.* **2006**, *97*, 055901.

(82) Dutt, G. B.; Doraiswamy, S. *J. Chem. Phys.* **1992**, *96*, 2475.

(83) Poole, P. H.; Grande, T.; Angell, C. A.; McMillan, P. F. *Science* **1997**, *275*, 322.

(84) Pollack, G. L. *Phys. Rev. A* **1981**, *23*, 2660.

(85) Pollack, G. L.; Enyeart, J. J. *Phys. Rev. A* **1985**, *31*, 980.

(86) Cicerone, M. T.; Ediger, M. D. *J. Chem. Phys.* **1996**, *104*, 7210.

(87) Swallen, S. F. *Phys. Rev. Lett.* **2003**, *90*, 015901.

(88) Ehlich, D.; Sillescu, H. *Macromolecules* **1990**, *23*, 1600.

(89) Voronel, A.; Veliyulin, E.; Machavariani, V. S.; Kisliuk, A.; Quitmann, D. *Phys. Rev. Lett.* **1998**, *80*, 2630.

(90) Tanaka, H. *J. Chem. Phys.* **2000**, *112*, 799.

(91) Li, J.; Wang, I.; Fayer, M. D. *J. Phys. Chem. B* **2005**, *109*, 6514.